4784 *Chem. Mater.* **2009,** *21,* 4784–4795
DOI:10.1021/cm901006g

CHEMISTRY OF MATERIALS
Article

Novel Phosphonate-Functional Poly(ethylene oxide)-Magnetite Nanoparticles Form Stable Colloidal Dispersions in Phosphate-Buffered Saline

J. D. Goff,[†,‡] P. P. Huffstetler,[†,‡] W. C. Miles,[†,§] N. Pothayee,[†,‡] C. M. Reinholz,[†,‡] S. Ball,[†] R. M. Davis,[†,§] and J. S. Riffle*[,†,‡]

[†]*Macromolecules and Interfaces Institute and* [‡]*Department of Chemistry and* [§]*Department of Chemical Engineering, Virginia Tech, Blacksburg, Virginia 24061*

Received April 11, 2009. Revised Manuscript Received September 15, 2009

Many studies have concerned the colloidal stability of magnetite nanoparticles coated with poly(ethylene oxide) (PEO), but their long-term stability when such complexes are exposed to physiological media is still not well understood. This paper describes effects of different functional anchor groups, including one carboxylate, one ammonium, one phosphonate zwitterion, and three phosphonate zwitterions, on the structural stabilities of PEO−magnetite nanoparticle complexes in water and phosphate buffered saline (PBS). While PEO oligomers bound to the magnetite through any of these functional groups remain stably bound in water, only the complexes with polymers bound through the zwitterionic phosphonates were stable in PBS. The stabilities of the PEO-magnetite complexes with these phosphonate zwitterions in PBS allowed for investigating colloidal properties of their dispersions as functions of the number of phosphonates per chain and the chain densities and molecular weights. In contrast to all of the other complexes studied, PEO−magnetite nanoparticles bound through three phosphonate zwitterions on one end of the PEO exhibited no significant change in size for over 24 h even when they were dispersed in PBS. The colloidal properties of all of these dispersions are discussed in light of their compositions and structures.

Introduction

Magnetite nanoparticles coated with biocompatible macromolecules have been of great interest due to a wide range of potential biomedical applications including drug delivery, treatment of detached retinas, cell separations and contrast enhancement agents for MRI.[1−6] PEO has been one of the most widely used coatings for magnetite nanoparticles because of its low cytotoxicity, ability to mask foreign substrates from the immune system, and FDA approval for in vivo applications.[1,7,8] Despite the prevalence of PEO as a coating for magnetite, there is a need to improve upon the binding efficacy of the polymer to the magnetite surface so that the materials will remain intact in physiological media.[9−11]

Functional anchor groups on polymers can aid in their adsorption to the surface of magnetite. Polymeric magnetite dispersion stabilizers containing carboxylate and alkylammonium anchor groups have been previously reported.[8,11−17] Over the past few decades, significant effort has been devoted to the surface modification of magnetite with PEO-containing polymers to improve

*Corresponding author.

(1) Bronich, T. N.; Nyugen, H. K.; Eisenberg, A.; Kabanov, A. V. *J. Am. Chem. Soc.* **2000**, *122*, 8339–8343.
(2) Jung, C. J. P. *Magn. Reson. Imaging* **1995**, *13*, 661–674.
(3) Mefford, O. T.; Carroll, M. R. J.; Vadala, M. L.; Goff, J. D.; Mejia-Ariza, R.; Saunders, M.; Woodward, R. C.; St. Pierre, T. G.; Davis, R. M.; Riffle, J. S. *Chem. Mater.* **2008**, *20*, 2184–2191.
(4) Mefford, O. T.; Vadala, M. L.; Goff, J. D.; Carroll, M. R. J.; Mejia-Ariza, R.; Caba, B. L.; St. Pierre, T. G.; Woodward, R. C.; Davis, R. M.; Riffle, J. S. *Langmuir* **2008**, *24*, 5060–5069.
(5) Thunemann, A. F.; Schutt, D.; Kaufner, L.; Pison, U.; Mohwald, H. *Langmuir* **2006**, *22*, 2351–2357.
(6) Wilson, K. S.; Goff, J. D.; Riffle, J. S.; Harris, L. A.; St. Pierre, T. G. *Polym. Adv. Technol.* **2005**, *16*, 200–211.
(7) Kabanov, A. V.; Zhu, J.; Alakhov, V. *Adv. Genet.* **2005**, *53*, 231–261.
(8) Harris, L. A.; Goff, J. D.; Carmichael, A. Y.; Riffle, J. S.; Harburn, J. J.; St. Pierre, T. G.; Saunders, M. *Chem. Mater.* **2003**, *15*, 1367–1377.
(9) Miles, W. C.; Goff, J. D.; Huffstetler, P. P.; Reinholz, C. M.; Pothayee, N.; Caba, B. L.; Boyd, J. S.; Davis, R. M.; Riffle, J. S. *Langmuir* **2009**, *25*, 803–813.
(10) Alexandridis, P. H.; Sakai, T. *Colloid Surf., A* **1995**, *96*, 1–46.
(11) Huffstetler, P. P.; Miles, W. C.; Goff, J. D.; Reinholz, C. M.; Carroll, M. R. J.; Woodward, R. C.; St. Pierre, T. G.; Davis, R. M.; Riffle, J. S. *Polym. Prepr.* **2008**, *49*, 1103–1104.
(12) Avelino, S. R.; Oliveira, F. M. L.; Oliveira, A. C.; Morais, P. C. *J. Non-Cryst. Solids* **2006**, *352*, 3692–3696.
(13) Cintra, E. R.; Santos, J. L. Jr.; Socolovsky, L. M.; Buske, N.; Bakuzis, A. F. *J. Magn. Magn. Mater.* **2008**, *320*, 351–353.
(14) Gravina, P. P.; Bakuzis, A. F.; Neto, K. S.; Azevedo, R. B.; Morais, P. C. *J. Magn. Magn. Mater.* **2005**, *289*, 448–451.
(15) Oliveira, F. M. L.; Avelino, S. R.; Eloi, M. T. A.; Gravina, P. P.; Neto, K. S.; Lima, E. C. D.; Morais, P. C. *J. Non-Cryst. Solids* **2006**, *352*, 3689–3691.
(16) Oliveira, F. M. L.; Canizares, A. P.; Figueiredo, L. C.; Neto, K. S.; Morais, P. C. *J. Appl. Phys.* **2009**, *105*, 33906–33909.
(17) Vadala, M. L.; Thompson, M. S.; Ashworth, M. A.; Lin, Y.; Vadala, T. P.; Ragheb, R.; Riffle, J. S. *Biomacromolecules* **2008**, *9*, 1035–1043.

Published on Web 09/30/2009

their biocompatibility, resist protein adsorption and increase their circulation time within the body.[1,7,18,19] Previous work by others has shown the capacity to coat magnetite nanoparticles with polymers containing pendant carboxylate groups, as well as with carboxylate, alkylammonium, or methoxysilane termini.[5,8,20−26] Investigations of the colloidal stabilities of magnetite and maghemite nanoparticles having organic coatings have been conducted in water and in saline (e.g., sodium chloride).[12−16,21,27] Stabilities of these complexes in water and saline were adequate, but the issue of their stabilities in media simulating physiological conditions that contain phosphate salts has received little attention. One interesting exception is that Chahana and Wang et al. recently reported magnetite nanoparticles coated with a hydrophilic polyacrylate that was bound through catechol moieties, and this was stable in PBS.[27]

This paper describes the synthesis of PEO oligomers containing functional anchor groups at one end (one carboxylate, one ammonium, one phosphonate zwitterion, three phosphonate zwitterions) and their adsorption onto magnetite nanoparticles. Relationships between the chemical nature of the anchor group(s) and the capacity to remain firmly bound to the magnetite, as well as the colloidal dispersion properties of the PEO−magnetite complexes, were studied in water and in PBS. Additionally, the influence of PEO molecular weight on colloidal properties of the PEO−magnetite complexes with similar polymer loadings has been investigated.

Experimental Section

Materials. Azobisisobutyronitrile (AIBN), benzyl alcohol (>98%), diethyl ether, diethyl vinyl phosphonate (97%), ethylene oxide (EO, 99.5+%), hexanes (HPLC grade), iron(III) acetylacetonate ($Fe(acac)_3$), mercaptoacetic acid (97+%), oleic acid (90%, technical grade), sodium iodide (99%), triethylamine (TEA, 99.5%), and 1.0 M vinylmagnesium bromide in THF were purchased from Aldrich and used as received. Tetrahydrofuran (THF, Optima grade, EMD Science, 99.5%) was refluxed over sodium metal with benzophenone until the solution reached a deep purple, fractionally distilled, and deoxygenated just prior to use. Glacial acetic acid (EMD Science) was diluted with THF, yielding a 2.0 M acetic acid solution. Naphthalene (Aldrich) was sublimed prior to use. Bromotrimethylsilane (TMS-Bromide, 97%) and mercaptoethylamine hydrochloride were purchased from Alfa Aesar and used as received. Ethanol (Decon Laboratories Inc.) was used as received. Methanol (HPLC grade), chloroform (HPLC grade), *N*,*N*-dimethylformamide (DMF, Optima grade), dichloromethane (HPLC grade), sodium bicarbonate, ammonium chloride, sodium chloride, and acetone (HPLC grade) were purchased from Fisher Scientific and used as received. 3-Chloropropyldimethylchlorosilane and 3-chloropropyltrichlorosilane were purchased from Gelest and used as received. Dialysis tubing (25 000 g mol^{-1} MWCO and 1000 g mol^{-1} MWCO) was obtained from Spectra/Por. Phosphate buffered saline 10X (PBS) was obtained from Lonza and diluted to appropriate concentrations.

Synthesis. *Synthesis of 3-Hydroxypropyldimethylvinylsilane (3-HPMVS) and 3-Hydroxypropyltrivinylsilane (3-HPTVS).* 3-HPMVS and 3-HPTVS were prepared utilizing a modified procedure originally developed by Vadala et al.[11,17] The procedure described herein that was utilized to prepare 3-HPMVS can be applied to the synthesis of 3-HPTVS with appropriate substitution of the trivinylsilane as the starting reagent. 3-Chloropropyldimethylchlorosilane (10.0 g, 0.06 mol) was syringed into a clean, flame-dried, two-neck, round-bottom flask equipped with a stir bar under a N_2 purge. The reaction flask was placed in an ice bath and cooled to 0 °C. A 1.0 M solution of vinylmagnesium bromide (64.0 mL, 0.064 mol) in THF was slowly added to the flask over 30 min. The flask was allowed to warm to room temperature, and the mixture was stirred for 24 h. The reaction mixture was diluted with dichloromethane (100 mL), transferred to a separatory funnel and washed with a saturated aqueous ammonium chloride solution (150 mL), and then the organic layer was further washed with aqueous sodium chloride (3 × 150 mL). Magnesium sulfate was added to the organic layer to remove any residual water, followed by vacuum filtration. Dichloromethane was removed under vacuum and the product was distilled at 100 °C, 0.8 Torr, yielding 3-chloropropyldimethylvinylsilane (8.91 g, 0.06 mol) (3-CPMVS). ^{1}H NMR was used to confirm the quantitative addition of vinyl groups.

3-CPMVS (8.91 g, 0.06 mol) was placed in a 250 mL round-bottom flask equipped with a stir bar and condenser. In a separate round-bottom flask, sodium iodide (16.4 g, 0.11 mol) was dissolved in acetone (60 mL) and the solution was syringed into the flask. The mixture was heated at 56 °C for 24 h. Acetone was removed under a vacuum and the product was dissolved in dichloromethane (100 mL) and vacuum filtered to remove the salt byproduct. Dichloromethane was removed under vacuum and the product was distilled at 100 °C, 0.8 Torr, yielding 3-iodopropyldimethylvinylsilane (3-IPMVS, 13.4 g, 0.05 mol). ^{1}H NMR confirmed the expected structure.

3-IPMVS (13.4 g, 0.05 mol) was placed in a 250 mL round-bottom flask equipped with a stir bar and condenser. DMF (20 mL) was added to the reaction flask followed by sodium bicarbonate (8.8 g, 0.10 mol) and DI water (5 mL). The mixture was heated to 100 °C for ∼24h and conversion of the alkyl iodide to an alcohol was monitored via ^{1}H NMR. The reaction mixture was transferred to a separatory funnel and washed 3× with DI water to remove the excess sodium bicarbonate and DMF. The liquid product floats on top of the aqueous DMF phase in these extractions. The product was fractionally distilled at 90 °C, 0.8 Torr, yielding 3-hydroxypropyldimethylvinylsilane (3-HPMVS, 7.4 g, 0.048 mol, 95% yield). ^{1}H NMR confirmed the expected chemical structure.

(18) Andrade, J.; Hlady, V.; Jeon, S. *Hydrophilic Polymers: Performance with Environmental Acceptance*; Advances in Chemistry Series; American Chemical Society: Washington, D.C., 1996; Vol. *248*, pp 51−59.
(19) Deen, W. M. *Analysis of Transport Phenomena*; Topics in Chemical Engineering; Oxford University Press: Oxford, U.K., 1998.
(20) Bica, D.; Vekas, L.; Avdeev, M.; Marinica, O.; Socolluc, V.; Balasolu, M.; Garamus, M. *J. Magn. Magn. Mater.* **2007**, *311*, 17–21.
(21) Park, J. Y.; Choi, E. S.; Baek, M. J.; Lee, G. H. *Mater. Lett.* **2009**, *63*, 379–381.
(22) Storm, G.; Belloit, S.; Daemen, T.; Lasic, D. *Adv. Drug Delivery Rev.* **1995**, *17*, 31–48.
(23) Jain, T. K.; Morales, M. A.; Sahoo, S. K.; Leslie-Pelecky, D. L.; Labhasetwar, V. *Mol. Pharm.* **2005**, *2*, 194–205.
(24) Thompson, M. S.; Vadala, T. P.; Vadala, M. L.; Lin, Y.; Riffle, J. S. *Polymer* **2008**, *49*, 345–373.
(25) Zhang, Q. A.; Thompson, M. S.; Carmichael-Baranauskas, A. Y.; Caba, B. L.; Zalich, M. A.; Lin, Y. N.; Mefford, O. T.; Davis, R. M.; Riffle, J. S. *Langmuir* **2007**, *23*, 6927–6936.
(26) Zhang, Y.; Kohler, N.; Zhang, M. *Biomaterials* **2002**, *23*, 1553–1561.
(27) Chanana, M.; Jahn, S.; Georgieva, R.; Lutz, J.; Baumler, H.; Wang, D. *Chem. Mater.* **2009**, *21*, 1906–1914.

Synthesis of Dimethylvinylsilyl-Functional PEO-OH (*dimethylvinylsilyl-PEO-OH*). A representative procedure for synthesizing a dimethylvinylsilyl-PEO-OH is provided. An 8300 g mol^{-1} M_n PEO oligomer was initiated with 3-HPMVS. A 300 mL, high-pressure Series 4561 Parr reactor was utilized for the polymerizations. EO (10.0 g, 0.23 mol) was distilled from a lecture bottle into the pressure reactor cooled with an isopropanol-dry ice bath. THF (5 mL) was added to the reactor via syringe. A potassium naphthalide solution was prepared by charging naphthalene (14.1 g, 0.11 mol) into a 250 mL, flame-dried, round-bottom flask equipped with a glass stir bar. Dry THF (100 mL) was syringed into the flask to dissolve the naphthalene. Potassium metal (3.96 g, 0.10 mol) was added to the solution followed by a N_2 purge for 30 min. The solution was stirred overnight and titrated with 1 N HCl to determine the molarity of the potassium naphthalide solution, which was shown to be 0.95 M. An initiator solution consisting of 3-HPMVS (0.19 g, 1.29 mmol), THF (5 mL) and potassium naphthalide (1.26 mL of a 0.95 M solution in THF, 1.20 mmol) was prepared in a separate flame-dried, 100 mL, round-bottom flask. The initiator solution was added to the stirring reaction mixture via syringe. The cooling bath was removed, and the reaction mixture was allowed to reach room temperature and maintained for 24 h. The polymerization was terminated by adding acetic acid (0.66 mL of a 2.5 M solution in THF, 1.65 mmol) to the pressure reactor via syringe. The pressure reactor was purged with N_2 for 1 h and then opened; its contents were transferred to a 250 mL round-bottom flask. The solvent was removed under a vacuum at room temperature, and the product was dissolved in 200 mL of dichloromethane. The product was washed twice with DI water (2 × 100 mL). The solution was concentrated under a vacuum at room temperature and precipitated in cold diethyl ether.

Synthesis of Trivinylsilyl-Functional PEO-OH (*trivinylsilyl-PEO-OH*). An exemplary procedure for synthesizing a trivinylsilyl-PEO−OH oligomer is provided. A 9 100 g mol^{-1} M_n PEO oligomer was initiated with 3-HPTVS in a 300 mL, high-pressure Series 4561 Parr reactor. EO (10.0 g, 0.23 mol) was distilled from a lecture bottle into the pressure reactor cooled with an isopropanol-dry ice bath (−30 °C), followed by addition of THF (5 mL) via syringe. A potassium naphthalide solution was prepared by charging naphthalene (14.1 g, 0.11 mol) into a 250 mL, flame-dried, round-bottom flask equipped with a glass stir bar. Distilled THF (100 mL) was syringed into the flask to dissolve the naphthalene. Potassium metal (3.96 g, 0.10 mol) was added to the solution followed by a N_2 purge for 30 min. The solution was stirred overnight and titrated with 1 N HCl to determine the molarity of the potassium naphthalide solution, which was shown to be 0.97 M. An initiator solution consisting of 3-HPTVS (0.19 g, 1.12 mmol), THF (5 mL) and potassium naphthalide (1.03 mL of a 0.97 M solution in THF, 1.0 mmol) was prepared in a separate flame-dried, 100-mL, round-bottom flask. The initiator solution was added to the stirring pressure reactor mixture via syringe. The dry ice/isopropanol bath was removed, and the reaction mixture was allowed to reach room temperature and maintained for 24 h. The polymerization was terminated by adding acetic acid (0.66 mL of a 2.5 M solution in THF, 1.65 mmol) to the pressure reactor via syringe. The pressure reactor was purged with N_2 for 1 h, then opened and its contents were transferred to a 250 mL round-bottom flask. The solvent was removed under vacuum at room temperature, and the product was dissolved in 200 mL of dichloromethane and washed twice with DI water (2 × 100 mL). The solution was concentrated under a vacuum at room temperature and precipitated in cold diethyl ether.

Functionalization of Dimethylvinylsilyl-PEO-OH with Carboxylic Acid Groups. An exemplary procedure for adding a carboxylic acid group via ene-thiol free radical chemistry across the vinylsilyl end group is provided for an 8300 g mol^{-1} dimethylvinylsilyl-PEO−OH. Dimethylvinylsilyl-PEO−OH (1.0 g, 0.12 mmol) was charged to a 100 mL round-bottom flask equipped with a stir bar and dissolved in 2 mL of deoxygenated toluene. Mercaptoacetic acid (37.0 mg, 0.36 mmol) was syringed into the reaction flask followed by the addition of AIBN (9.2 mg, 0.06 mmol) dissolved in 0.5 mL of toluene. The mixture was deoxygenated for 10 min by sparging with N_2, and then reacted at 80 °C for 24 h. The reaction mixture was dissolved in 200 mL of dichloromethane, transferred to a separatory funnel, and washed with DI water 3× to remove the excess mercaptoacetic acid. The dichloromethane was removed via rotary evaporation and the resulting polymer was precipitated into cold diethyl ether. The polymer was dried at room temperature under a vacuum for 24 h, yielding 0.94 g of carboxylic acid-functionalized PEO.

Functionalization of Dimethylvinylsilyl-PEO-OH or Trivinylsilyl-PEO-OH with Ammonium Group(*s*). Heterobifunctional polyethers with a terminal ammonium group (ammonium-PEO−OH) were obtained via ene-thiol addition of mercaptoethylamine hydrochloride across the vinylsilane. In a characteristic procedure, an 8300 g mol^{-1} dimethylvinylsilyl-PEO−OH (2 g, 0.24 mmol), mercaptoethylamine hydrochloride (45.2 mg, 0.4 mmol), and AIBN (20 mg, 0.12 mmol) were dissolved in deoxygenated DMF (5 mL) in a 100 mL round-bottom flask equipped with a stir bar. The reaction was conducted at 70 °C for 24 h with stirring, and then the reaction mixture was cooled to room temperature. DI water (100 mL) was added to the flask, and the mixture was transferred to a separatory funnel. Dichloromethane (200 mL) was added to the separatory funnel to extract the alkylammonium-functionalized polyether from the water layer. The dichloromethane layer was washed with a 1 N solution of sodium bicarbonate (3×), followed by 3 washes with DI water. The dichloromethane solution was concentrated under a vacuum, and the ammonium-PEO-OH oligomer was precipitated into cold diethyl ether and dried at 25 °C under a vacuum for 12 h, yielding 1.9 g of product (95% yield).

A PEO oligomer with three ammonium groups on one end (ammonium$_3$-PEO-OH) was prepared by a similar procedure using trivinylsilyl-PEO-OH as the starting substrate, and the same molar ratios of reagents to equivalents of vinyl groups as described above.

Michael Addition of Ammonium-PEO-OH or Ammonium$_3$-PEO-OH onto Diethyl Vinyl Phosphonate. A characteristic procedure for adding a phosphonate group to an 8300 g mol^{-1} ammonium-PEO-OH is provided. An ammonium-PEO-OH oligomer (1.0 g, 0.12 mmol) was charged to a clean, flame-dried, 100 mL, round-bottom flask equipped with a stir bar, and dissolved in ethanol (9 mL). TEA (0.20 mL, 0.14 mmol) was added to the reaction, followed by diethyl vinyl phosphonate (0.26 mL, 0.14 mmol). The reaction was carried out at 70 °C for 24 h. The reaction mixture was diluted with DI water to obtain a 75:25 water:ethanol composition and placed in a 1000 g mol^{-1} MWCO cellulose acetate dialysis bag and dialyzed against 4 L of DI water for 24 h to remove excess diethyl vinyl phosphonate. The contents of the dialysis bag were transferred to a 100 mL round-bottom flask and lyophilized, yielding 0.91 g of diethyl phosphonate-functionalized PEO.

A PEO oligomer with three phosphonate groups on one end (phosphonate$_3$-PEO-OH) was prepared by a similar procedure

using ammonium$_3$-PEO-OH as the starting substrate, and the same molar ratios of reagents to equivalents of ammonium groups as described above.

Hydrolysis of Diethylphosphonate-PEO-OH (or diethylphosphonate$_3$-PEO-OH) Yielding Phosphonic Acid-PEO-OH (or phosphonic acid$_3$-PEO-OH). Phosphonic acid-PEO-OH was prepared from diethyl phosphonate-PEO-OH using a hydrolysis procedure adapted from Caplan et al.[28] In a representative procedure, an 8300 g mol^{-1} diethyl phosphonate-PEO-OH (0.80 g, 0.10 mmol) was charged to a clean, 100 mL round-bottom flask equipped with a stir bar and dissolved in 5 mL of dichloromethane. Trimethylsilyl bromide (0.032 mL, 0.24 mmol) was syringed into the reaction flask and stirred at room temperature for 24 h. Methanol (0.01 mL, 0.24 mmol) was added and stirred for 2 h to cleave the trimethylsilyl groups. Dichloromethane (50 mL) was added, and the mixture was washed 3× with DI water (100 mL each) in a separatory funnel. The dichloromethane layer was concentrated, then the oligomer was precipitated by pouring the mixture into cold diethyl ether. The polymer was vacuum-dried at 25 °C for 24 h, yielding 0.77 g of phosphonic acid-PEO-OH.

A PEO oligomer with three phosphonate groups on one end (phosphonate$_3$-PEO-OH) was prepared by a similar procedure using diethylphosphonate$_3$-PEO-OH as the starting substrate, and the same molar ratios of reagents to equivalents of phosphonate groups as described above.

Magnetite Synthesis via Reduction of Fe(acac)$_3$. Magnetite nanoparticles were synthesized using a reduction method adapted from Pinna et al.[29] Fe(III) acetylacetonate (2.14 g, 8.4 mmol) and benzyl alcohol (45 mL, 0.43 mol) were charged to a 250 mL, three-neck, round-bottom flask equipped with a water condenser and placed in a Belmont metal bath with an overhead stirrer with both thermostatic (±1 °C) and revolution per minute control. The solution was sparged with N_2 for 1 h. While stirring under N_2 at 300 rpm, the solution was heated at 100 °C for 4 h, and the temperature was then increased to 205 °C at a rate of ~25 °C h^{-1}. Following 24 h at 205 °C, the reaction was cooled to room temperature; the magnetite particles were then collected with a magnet and the benzyl alcohol was decanted. The magnetite nanoparticles were washed 3× with acetone (100 mL each), then were dispersed in chloroform (20 mL) containing oleic acid (0.3 g). The solvent was removed under vacuum at room temperature, and the oleic acid-stabilized magnetite nanoparticles were washed 3× with acetone (100 mL each). The particles were dried under a vacuum for 24 h at 25 °C. The composition of the particles obtained from thermogravimetric analysis (TGA) was 5% organic residue to 95% magnetite.

Adsorption of Functional Polyether Stabilizers onto Magnetite Nanoparticles. A representative method for preparing a targeted composition of 70:30 wt:wt polyether:magnetite complex is provided. Oleic acid-stabilized magnetite nanoparticles (50.0 mg) prepared as described above were dispersed in chloroform (10 mL) and charged to a 50 mL round-bottom flask. A functional PEO (117.0 mg) was dissolved in chloroform (10 mL) and added to the dispersion. The pH of each solution and the resulting mixture were approximately neutral. The reaction mixture was sonicated in a VWR 75T sonicator for 16 h under N_2, and the nanoparticles were then precipitated in hexanes (300 mL). A magnet was utilized to collect the magnetite nanoparticles and free oleic acid was decanted with the supernatant. The complexes were dispersed in DI water (20 mL) using sonication for 30−60 s. The complexes were dialyzed against DI water (4 L) for 24 h using 25 000 g mol^{-1} MWCO dialysis bags.

Characterization. ^{1}H NMR spectral analyses of compounds were performed using a Varian Unity 400 NMR or a Varian Inova 400 NMR operating at 400 MHz.

An Alliance Waters 2690 Separations Module with a Viscotek T60A dual viscosity detector and laser refractometer equipped with a Waters HR 0.5 + HR 2 + HR 3 + HR 4 styragel column set was used for gel permeation chromatography (GPC) analyses. GPC data were collected in chloroform at 30 °C. Data were analyzed utilizing a Universal calibration made with polystyrene standards to obtain absolute molecular weights.

TGA was used to determine the polymer loading for each complex. TGA measurements were carried out on the PEO-magnetite nanoparticles using a TA Instruments TGA Q500 to determine the fraction of each complex that was comprised of polymer. Freeze-dried samples were first held at 110 °C for 10 min to drive off any excess moisture. The samples (10−15 mg) were then equilibrated at 100 °C and the temperature was ramped at 10 °C min^{-1} to a maximum of 700 °C in a nitrogen atmosphere. The mass remaining was recorded throughout the experiment. The mass remaining at 700 °C was taken as the fraction of magnetite in the complexes. The experiments were conducted in triplicate.

DLS measurements were conducted with a Malvern Zetasizer NanoZS particle analyzer (Malvern Instruments Ltd., Malvern, UK) at a wavelength of 633 nm from a 4.0 mW, solid-state He−Ne laser at a scattering angle of 173° and at 25 ± 0.1 °C. Intensity, volume, and number average diameters were calculated with the Zetasizer Nano 4.2 software utilizing an algorithm, based on Mie theory, that transforms time-varying intensities to particle diameters.[30] For DLS analysis, the dialyzed complexes dispersed in DI water were diluted to ~0.05 mg mL^{-1} and filtered through a Whatman Anotop, 100 nm, alumina filter directly into a polystyrene cuvette. This corresponds to a volume fraction of 1.3×10^{-5} to 2.2×10^{-5} depending on the polymer loading on the magnetite. In experiments where PBS was added, 0.1 mL of 10X PBS was mixed with 0.9 mL of the 0.05 mg mL^{-1} complex solution, and the solution was then filtered through a 100 nm alumina filter into a clean polystyrene cuvette. Each sample was analyzed immediately following filtration and remeasured every 30 min over 24 h.

A 7T MPMS Squid magnetometer (Quantum Design) was used to determine magnetic properties. Hysteresis loops were generated for the magnetite nanoparticles at 300 and 5 K. Fe concentration of the magnetite was determined chemically by acid digestion followed by ICP-AES analysis. These concentrations were in good agreement with TGA values.

Results and Discussion

One primary issue regarding the structures of polymer−magnetite nanostructures for biomedical applications is the colloidal stability of dispersions of such complexes in physiological media.[9,10,25] The aim of this study has been to compare the binding efficacies of PEO oligomers with different functional anchoring groups to magnetite, particularly in the presence of phosphate salts, because these are present in physiological media. PEO oligomers with one terminal carboxylate, ammonium or a phosphonate

(28) Caplan, N. A.; Pogson, C. I.; Hayes, D. J.; Blackburn, G. M. *R. Soc. Chem.* **2000**, *1*, 421–437.
(29) Sun, Y.; Wang, B.; Hui, C.; Wang, H. P.; Jiang, J. M. *J. Macromol. Sci., Part B: Phys.* **2006**, *45*, 653–658.
(30) *Zetasizer Nano Series User Manual*; Malvern Instruments, Ltd.: Worcestershire. U.K., 2005.

zwitterion, and with three phosphonate zwitterions (all on one end of the PEO) were adsorbed onto magnetite nanoparticles, and the stabilities of the complexes were compared. Knowledge of which binding groups remained stably bound to the magnetite in water and in PBS then allowed us to examine the colloidal properties of the stable nanoparticle complexes in dispersions in light of the molecular weights and chain densities of the bound oligomers on the magnetite surfaces.

Synthesis of PEO oligomers with different functional end groups for binding to magnetite. 3-HPMVS was used as a versatile initiator for living anionic polymerizations of EO to produce heterobifunctional oligomers that could be postfunctionalized with the different chemical groups to adsorb onto the magnetite nanoparticles (Scheme 1).[17,24] This approach allowed for utilizing the same oligomer for comparing dispersion properties with the only difference being the functional anchor groups. A variation on this approach using 3-HPTVS as the initiator was also investigated to prepare phosphonate$_3$-PEO-OH oligomers, so that the dispersion properties could be compared with nanoparticles having different surface densities of functional binding groups. Potassium naphthalide was reacted with 3-HPMVS or 3-HPTVS to form an alkoxide for initiating EO, and the number of moles of the alcohol initiator relative to EO controlled the molecular weight. A small deficiency of the naphthalide relative to alcohol ensured that only the alkoxide (and not residual naphthalide) initiated the chains, and the remaining alcohol chains transferred protons with the growing PEO chains throughout the reaction. It is noteworthy that these polymerizations were terminated with acetic acid prior to opening the reaction vessel to avoid any unwanted oxidative side reactions.

Dimethylvinylsilyl-PEO-OH oligomers with targeted molecular weights of approximately 3,000 and 8,000 g mol^{-1} were prepared and the materials were characterized using ^{1}H NMR and GPC (Table 1). Figure 1 shows a representative NMR spectrum of a dimethylvinylsilyl-PEO−OH oligomer. Number average molecular weight was determined by comparing the integral ratios of the resonances corresponding to the methylene groups in the initiator (labeled 3 and 4) to the repeat unit of ethylene oxide labeled 6. GPC of the dimethylvinylsilyl-functional polyethers revealed symmetric monomodal peaks with molecular weight distributions of less than 1.1, which are indicative of living anionic polymerizations (Figure 2). Good molecular weight agreement was found between both methods of analysis.

Ene-thiol additions were utilized to introduce carboxylate and ammonium end groups onto the polyethers (Scheme 2). The vinylsilyl functionality is unusual among vinyl groups in that it does not polymerize readily by free radical reactions, and thus it is seemingly an ideal substrate for ene-thiol functionalization reactions because polymerization does not compete. Nevertheless, excesses of the thiol relative to vinylsilane were utilized for these reactions to ensure quantitative addition.

Scheme 1. Synthesis of Dimethylvinylsilyl-PEO-OH via Living Anionic Polymerization

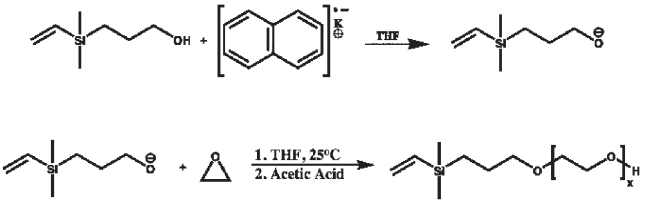

Table 1. Molecular Weights of Dimethylvinylsilyl-PEO-OH and Trivinylsilyl-PEO-OH Oligomers

	M_n (g mol^{-1})		
targeted molecular weight	^{1}H NMR	GPC	PDI[a]
monovinylsilyl-3000 g mol^{-1}	2900	3100	1.09
monovinylsilyl-8000 g mol^{-1}	8300	7900	1.05
trivinylsilyl-3000 g mol^{-1}	3400	3400	1.04
trivinylsilyl-9000 g mol^{-1}	9100	9500	1.09

[a] PDI = polydispersity index.

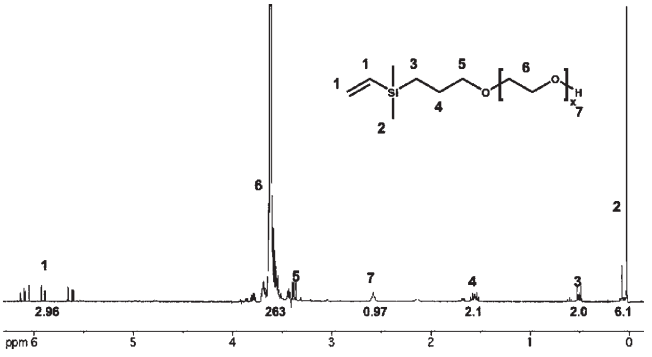

Figure 1. ^{1}H NMR of a 2,900 g mol^{-1} dimethylvinylsilyl-PEO-OH oligomer.

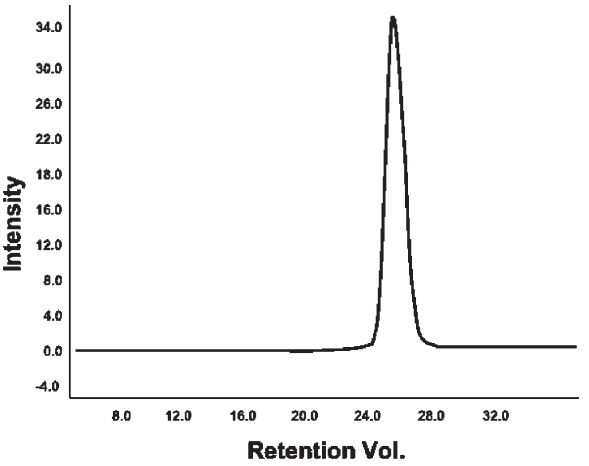

Figure 2. GPC chromatogram of a dimethylvinylsilyl-PEO-OH oligomer showing a M_n value of 7900 g mol^{-1} and a molecular weight distribution of 1.05.

Addition of mercaptoacetic acid to dimethylvinylsilyl-PEO−OH was monitored by ^{1}H NMR. Complete disappearance of the vinyl group at ~6 ppm indicated stoichiometric conversion to a carboxylic acid-PEO−OH (Figure 3A). Additionally, appearances of the methylene peaks labeled 1−3 in the spectrum indicated addition

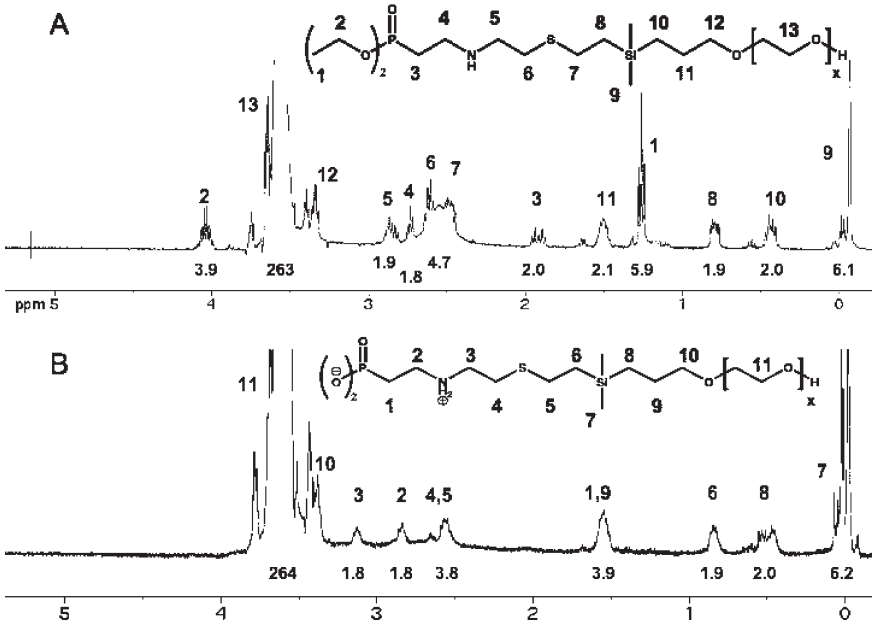

Figure 3. Ene-thiol addition of (A) mercaptoacetic acid and (B) 2-mercaptoethylamine hydrochloride to a 2900 g mol^{-1} polyether, yielding carboxylic acid and ammonium-functionalized PEO oligomers.

Scheme 2. Ene-thiol Additions of 2-Mercaptoethylamine Hydrochloride (R_1) and Mercaptoacetic Acid (R_2) to Dimethylvinylsilyl-PEO-OH

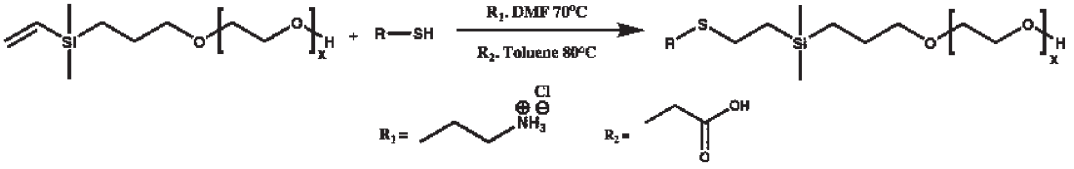

of mercaptoacetic acid. Comparison of the resonance integrals corresponding to the methylene peaks of the thiol (1−3) to the methylene peak labeled 5 confirmed quantitative addition across the vinylsilane end groups.

^{1}H NMR was also utilized to monitor ene-thiol addition of 2-mercaptoethylamine hydrochloride onto the vinylsilane end groups of dimethylvinylsilyl-PEO-OH and trivinylsilyl-PEO-OH by observing the complete disappearance of the vinyl groups and appearances of methylene peaks labeled 1−4 in the spectra (Figure 3B). Comparison of integrations confirmed quantitative functionalization with ammonium groups to form ammonium-PEO-OH or ammonium$_3$-PEO-OH.

The ammonium-functional PEO oligomers were used as precursors to form the zwitterionic phosphonate-functional polyethers. The ammonium end groups were first reacted with triethylamine to afford the corresponding free amines. A slight molar excess of triethylamine was added to maintain basic reaction conditions, aiding in nucleophilic addition to diethyl vinyl phosphonate. Diethyl vinyl phosphonate was added to the amine group(s) via Michael addition, yielding diethylphosphonate-PEO-OH (Scheme 3) or diethylphosphonate$_3$-PEO−OH utilizing a procedure adapted from the literature.[31]

Scheme 3. Michael Addition of Amine-PEO-OH to Diethyl Vinyl Phosphonate and De-esterification To Remove the Ethyl Groups Yielding Zwitterionic Phosphonate-PEO-OH

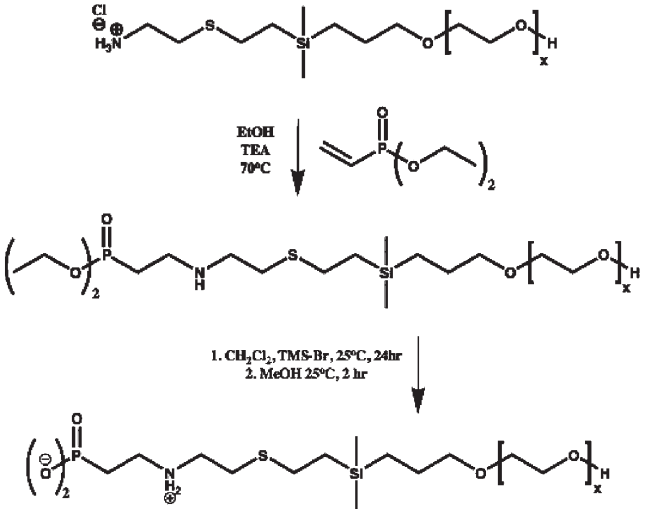

Figure 4A shows an ^{1}H NMR spectrum of a representative diethylphosphonate-PEO-OH oligomer. Two methylene peaks corresponding to the converted vinyl group of the phosphonate reactant are observed as peaks 3 and 4 in the spectrum of the product. Quantitative addition to diethyl vinyl phosphonate was determined by

(31) Jones, M., Jr. *Organic Chemistry*, 2nd ed.; W. W. Norton and Company: New York, 2000.

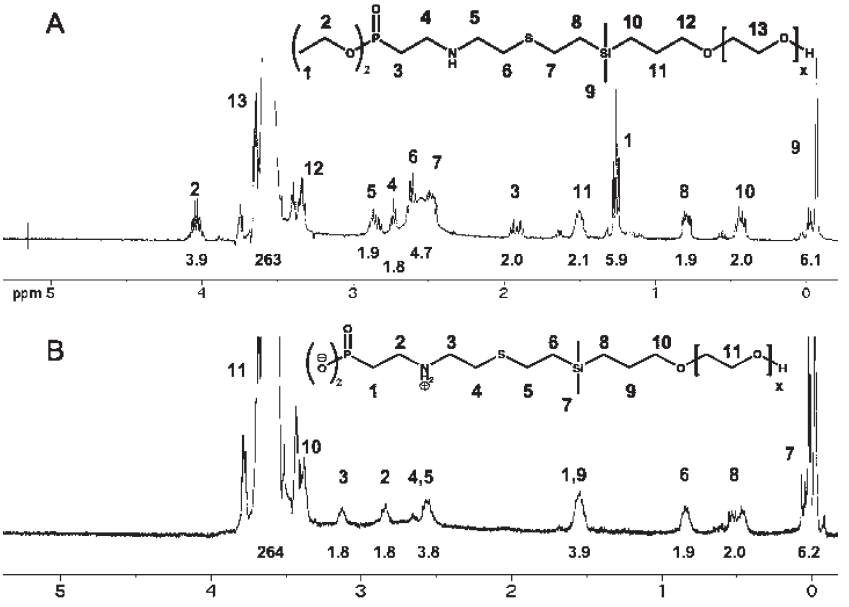

Figure 4. ^{1}H NMR of (A) a 2900 g mol^{-1} diethylphosphonate-PEO-OH and (B) a 2900 g mol^{-1} zwitterionic phosphonate-PEO-OH.

comparing the integrations of peaks 1−4 to the integration of the methylene peak labeled 10.

For binding to magnetite, the ethyl phosphonate groups were cleaved using bromotrimethylsilane (TMS-Br).[28] Reaction with TMS-Br yielded an intermediate bistrimethylsilyl ester with an alkyl halide byproduct. In the methanolysis step of the reaction, the alcohol cleaved the silyl ester, yielding phosphonic acid (Scheme 3). A zwitterionic end group was afforded in the phosphonate-PEO−OH product (or in the corresponding phosphonate$_3$-PEO-OH) at a pH less than ~10, due to the negative charge of the phosphonate(s) and the protonated secondary amine(s). ^{1}H NMR spectra confirmed that deprotection of the diethylphosphonate-PEO−OH oligomers was complete as shown in Figure 4B. In addition to the disappearance of the ethyl resonances in the spectrum, there was an upfield shift (~1.6 ppm) of the methylene group adjacent to the phosphorus atom.

Formation of PEO−magnetite Complexes via Adsorption of the Functional PEO Oligomers onto the Surfaces of Magnetite Nanoparticles. PEO-magnetite complexes with similar polymer loadings were formed with the two sets of different molecular weight PEO oligomers, then the complexes were dialyzed against water to remove any unbound PEO (Figure 5). Table 2 shows the polymer loadings in the complexes determined by TGA after dialysis and the number weighted average diameters in water as measured by dynamic light scattering (DLS). The compositions of the PEO−magnetite complexes were in close agreement with the targeted 30 wt % magnetite:70 wt % polyether composition. The PEO−magnetite complexes with the ammonium and zwitterionic phosphonate anchor groups had approximately the same number weighted average diameters, whereas the complexes with the carboxylate anchor groups were significantly smaller. The size of the magnetite nanoparticle core was measured via TEM with an average diameter of 8.1 ± 2.9 nm (Figure 6). The magnetic properties of the magnetite nanoparticles were characterized via superconducting quantum interference device analyses. Hysteresis loops revealed superparamagnetic behavior and a saturation magnetization of 80 emu g^{-1} of magnetite.

Determination of the Efficacies of Various Anchor Groups for Magnetite Nanoparticles in PBS. Binding of the polymers to the magnetite surfaces in PBS were studied to compare the stabilities of these complexes in a medium partially simulating physiological conditions. Dispersions of the complexes were dialyzed against PBS for 24 h to measure any polymer desorption that might be caused by displacement by salts in the medium. The complexes were subsequently dialyzed against water for an additional 24 h to remove any desorbed polymer and salts. TGA was used to determine the polymer loadings of the complexes before and after this process (Table 2). Desorption of the polymer from the magnetite surface in PBS was indicated by a decrease in polymer loading. Large decreases in polymer loadings (~25 wt %) were observed for the complexes bound through carboxylate or ammonium anchor groups. In addition, significant sedimentation of these complexes was observed during the PBS dialysis step, further substantiating instability in PBS. By contrast, no loss in polymer loading was observed for the complexes containing monozwitterionic phosphonate or trizwitterionic phosphonate anchor groups after PBS dialysis. These complexes also did not exhibit sedimentation in the PBS during the 24 h. On the basis of this study, it was reasoned that PEO−magnetite nanoparticles with the zwitterionic phosphonate anchor groups would likely have superior stability in physiological media in comparison to ammonium or carboxylate groups.

Investigation of Colloidal Stabilities of the PEO−Magnetite Nanoparticle Dispersions in Water and PBS Using DLS. Colloidal stabilities of the PEO-magnetite

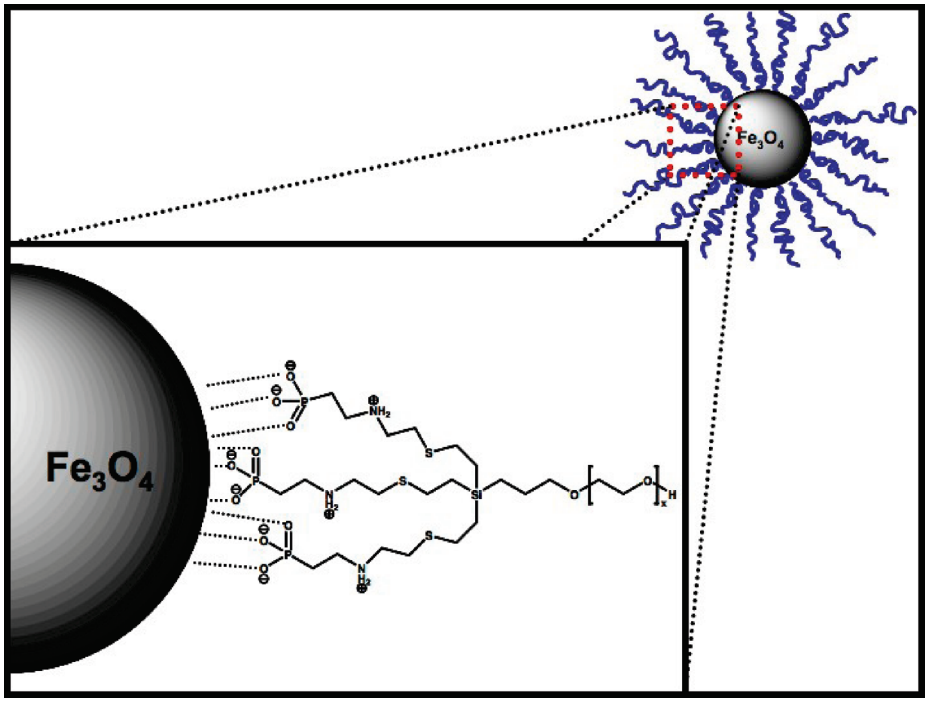

Figure 5. Depiction of a trizwitterionic phosphonate-PEO-OH binding to the surface of a magnetite nanoparticle.

Table 2. Compositions of the PEO−Magnetite Nanoparticle Complexes

PEO molecular weight (g mol^{-1})	anchor group(s)	Initial polymer loading after dialysis against H_2O (Wt %)	D_n (nm)	polymer loading after dialysis against PBS (wt %)
2900	mono-carboxylate	64.7 ± 0.9	19.9	40.7 ± 1.4
8300	mono-carboxylate	68.4 ± 1.6	24.5	45.3 ± 1.4
2900	mono-ammonium	66.8 ± 0.8	26.8	41.0 ± 0.7
8300	mono-ammonium	77.1 ± 0.9	31.7	42.6 ± 0.7
2900	mono-zwitterionic phosphonate	63.3 ± 0.4	26.2	65.1 ± 1.4
8300	mono-zwitterionic phosphonate	70.2 ± 0.7	39.6	67.7 ± 0.7
3400	tri-zwitterionic phosphonate	69.0 ± 0.6	27.6	68.8 ± 0.4
9100	tri-zwitterionic phosphonate	70.5 ± 0.8	34.2	69.2 ± 0.8

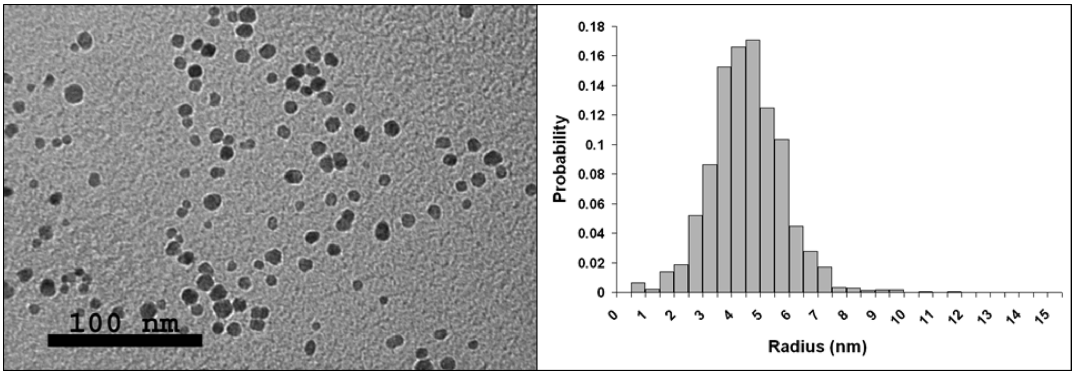

Figure 6. (A) TEM of the magnetite nanoparticles and (B) a histogram of the particle size distribution.

complexes against flocculation in DI water and PBS were examined using DLS by measuring the nanoparticle diameters every 30 min for 24 h. Figure 7 shows the diameters of the complexes containing the PEO oligomers with the monoammonium anchor group. Intensity weighted diameters are reported because of their sensitivity to the presence of aggregates (because they scale with radii to the sixth power), so that any agglomeration with time is magnified. Consistent with the desorption data, sizes of the ammonium−PEO−magnetite complexes did not change significantly over 24 h in water, whereas large increases in the diameters were observed for the complexes in PBS. Moreover, sediment was visually observed for the ammonium−PEO−magnetite complexes in PBS. Based on the calculation for the terminal velocity of a sphere (eq 1) in solution, these magnetite complexes should settle to the bottom of the DLS cuvette when an aggregate diameter of

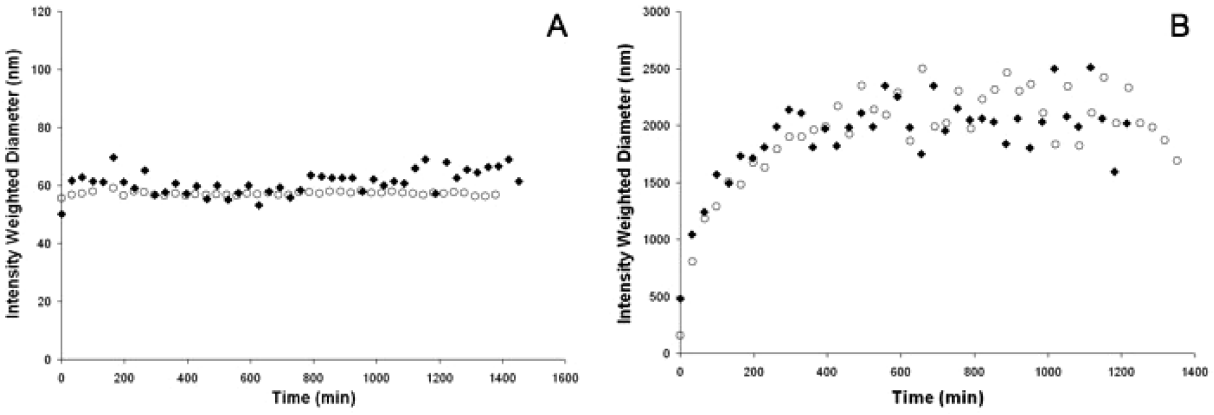

Figure 7. Intensity weighted diameters from DLS of the 2,900 (open circles) and 8300 g mol^{-1} (black diamonds) ammonium-PEO-magnetite complexes in (A) DI water and (B) PBS over 24 h.

~400−700 nm is reached[19]

$$U = \frac{2}{9}\frac{r^2 g(\rho_{mag} - \rho_{solvent})}{\mu_{solvent}} \quad (1)$$

Here, U is the terminal velocity of the particle, g is the gravitational constant, r is the particle radius, ρ_{mag} is the density of the magnetite complex (2.3 g mL^{-1}), $\rho_{solvent}$ is the density of the solvent, and $\mu_{solvent}$ is the viscosity of the solvent at 25 °C. Thus, after ~200 min in PBS, the ammonium−-PEO−magnetite complexes were likely on the verge of sedimentation and the sizes measured by DLS do not represent complexes that were at equilibrium in terms of size.

Magnetic characterization data shows that the magnetite nanoparticles display superparamagnetic behavior. The maximum potential energy of magnetic dipoles aligned with an applied magnetic field can be estimated by eq 2,[32]

$$V_M = \frac{8\pi\mu_o a^3 M^2}{9\left(\frac{h}{a}+2\right)^3} \quad (2)$$

Here, a is the particle radius, M is the magnetization, μ_o is the magnetite permeability in vacuum (1.26×10^{-6} T m/A), and h is the surface-to-surface separation of two particles. In the presence of the Earth's magnetic field (0.3−0.6 Gauss), any dipole−dipole interaction is significantly smaller than the van der Waal's interactions of the particles ($V_{vdW}/kT = 0.4$, $h = 5$ nm), even at particle sizes of 1000 nm ($V_M/kT = 2 \times 10^{-7}$, $h = 5$ nm) where the particles are settling out of suspension. Thus, van der Waal's forces would dominate and cause flocculation before any magnetic dipole−dipole interaction would become significant.

Figure 8 compares the diameters of the complexes containing the carboxylate anchor groups in DI water (A) and PBS (B and C). As expected, these complexes did not increase in intensity average diameter in DI water over time. However, flocculation was observed for the 8,300 g mol^{-1} carboxylate-PEO-magnetite complex in PBS over time, and the complexes with the 2900 g mol^{-1} PEO aggregated to ~100 nm in intensity weighted diameter with an equilibrium diameter reached after ~5 h. Thus, even with polymer desorption, the PEO molecular weight affects the behavior of these complexes in PBS. A possible explanation for this is the difference in numbers of polymer chains anchored to the magnetite nanoparticle surfaces in the two cases. Each complex has approximately the same polymer loading (~65 wt %), resulting in more total chains for the 2900 g mol^{-1} complexes (~3.0 chains nm^{-2}) relative to the 8300 g mol^{-1} complexes (~1.1 chains nm^{-2}). DLS data presented in Table 2 also shows that the complexes with carboxylate anchor groups have significantly smaller number weighted average diameters than their ammonium counterparts. The smaller diameters of the complexes with the carboxylate anchor groups reflect a higher local density of polymer near the magnetite surface. As reflected in Figures 7 and 8, the complexes with carboxylate anchor groups also flocculate less rapidly in PBS relative to the complexes with ammonium anchors. This can be partially attributed to the higher polymer density around the magnetite in the carboxylate case.

The relative colloidal stability of dispersions of these complexes with ammonium or carboxylate end groups in DI water versus PBS is consistent with the absence of polymer desorption in water and significant desorption in PBS. Based on previous work, it appears that phosphate salts from the PBS can displace these polymer anchor groups.[9] This reduces steric repulsion and promotes flocculation of the nanoparticles due to pair−pair van der Waal's interactions. Figure 9 illustrates adsorption of phosphate salts on the magnetite surface. In PBS, the magnetite nanoparticles cross the line of zero charge at ~pH 2.5, and this closely corresponds to the lowest pK_a of phosphonic acid. This suggests that phosphate salts from the PBS adsorb on the magnetite surfaces.

Figure 10 shows intensity-weighted diameters of complexes bound through the monozwitterionic phosphonate anchor groups in DI water (A) and PBS (B), where polymer desorption does not occur in either medium.

(32) Rosensweig, R. E. *Ferrohydrodynamics*; Cambridge University Press: Cambridge, U.K., 1985.

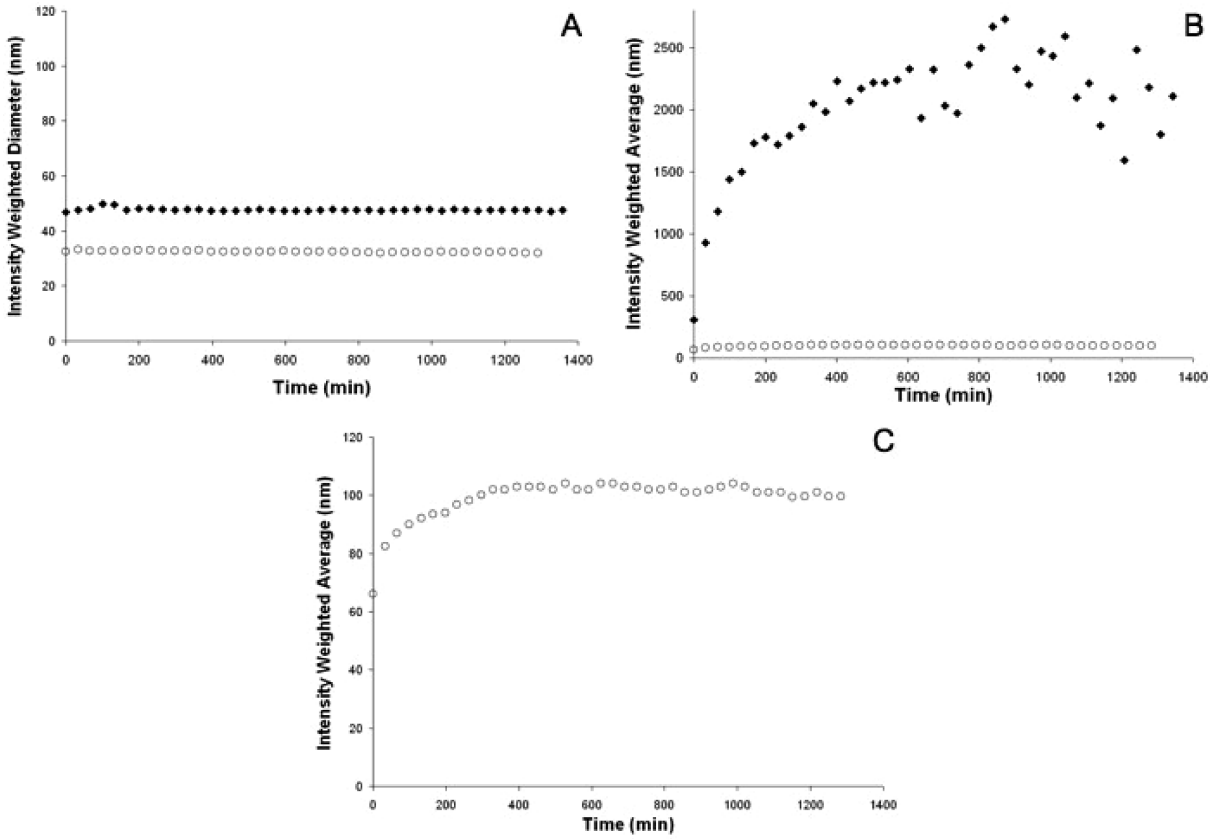

Figure 8. DLS intensity weighted diameters of the 2900 (open circles) and 8300 g mol^{-1} (black diamonds) of carboxylate-PEO-magnetite complexes in (A) DI water and (B) PBS over 24 h. A magnified plot of the 2900 g mol^{-1} carboxylate−PEO−magnetite complex in PBS is shown in (C).

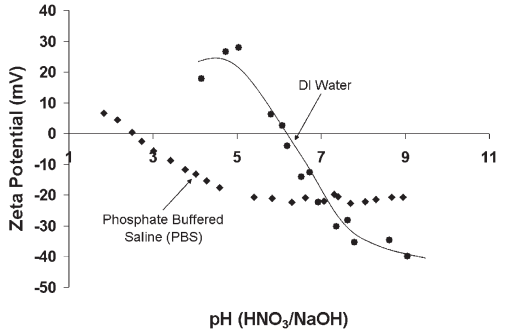

Figure 9. Zeta potentials indicate the charge characteristics of magnetite nanoparticle surfaces in DI water versus PBS.

To our surprise, although the sizes of some of these nanoparticles remained constant over time, some of them increased in size over time in both media, even without polymer desorption. The hydrodynamic sizes in PBS, however, remained significantly smaller than the analogous materials containing the carboxylate or ammonium anchors, and this result was deemed promising.

Figure 11 compares intensity-weighted diameters of the complexes containing the PEO with one phosphonate zwitterion anchor group over time in DI water and a 0.17 M NaCl solution (same ionic strength as the PBS). No difference in size was observed for the complex with the 2900 g mol^{-1} PEO in the salt solution, and better stability was observed for the 8300 g mol^{-1} complex in the salt solution. This indicates that it is not the ionic strength of the PBS that induces flocculation in these cases. The slight aggregation of the complex with the 8300 g mol^{-1} PEO in DI water appears to be due to attractive electrostatic forces that are screened when the complex is in 0.17 M NaCl. The reduction in Debye length with sodium chloride appears to reduce the electrostatic attraction. Additionally, the stability of the 2900 g mol^{-1} complex in DI water indicates that a denser polymer brush layer also prevents aggregation.

On the basis of the data discussed above, PEO−magnetite complexes containing one zwitterionic phosphonate anchor group showed significant improvement over the other anchor groups, but long-term colloidal stability was still not achieved. To address this issue, three phosphonate zwitterions, all on one end of the PEO oligomers, were investigated as anchor groups to probe any effect of cooperative binding and/or of each chain having a larger "footprint" on the magnetite surface. Figure 12 shows the intensity-weighted diameters of PEO−magnetite complexes bound through trizwitterionic phosphonates in (A) DI water and (B) PBS. Long-term colloidal size stability was observed for the 3400 and 9100 g mol^{-1} trizwitterionic phosphonate PEO-magnetite complexes in both media. Thus, at similar polymer loadings, three phosphonate anchor groups on the polymer chain end yielded complexes that did not undergo polymer desorption AND they did not aggregate over 24 h in PBS.

We hypothesize that the size stability of the zwitterionic phosphonate$_3$−PEO−magnetite complexes in PBS can be

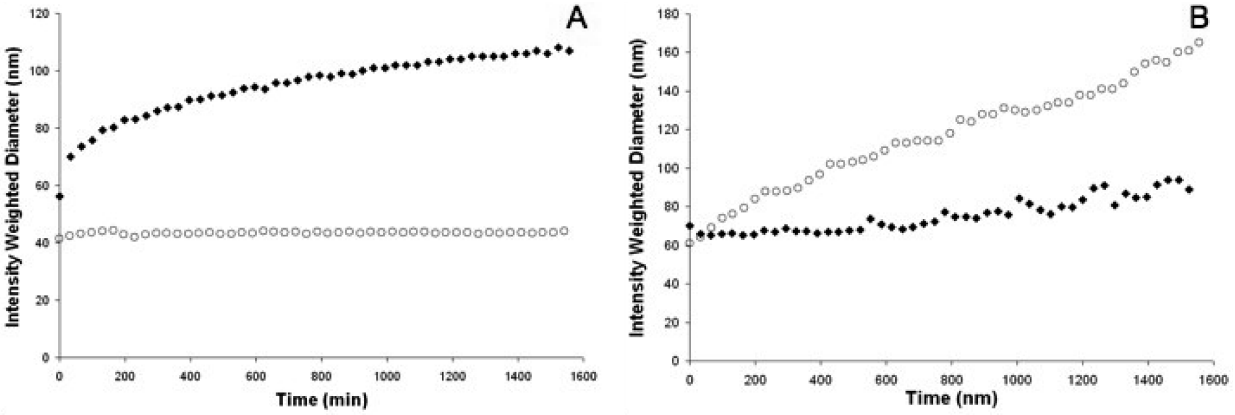

Figure 10. DLS intensity weighted diameters of the 2900 (open circles) and 8300 g mol^{-1} (black diamonds) monozwitterionic phosphonate−PEO−magnetite complexes in (A) DI water and (B) PBS over 24 h.

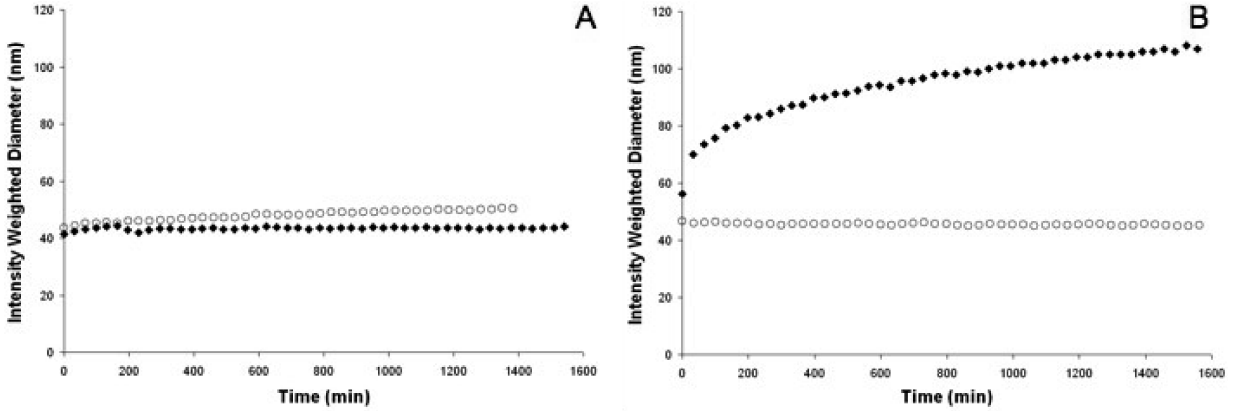

Figure 11. DLS intensity weighted diameters of (A) the 2900 g mol^{-1} monozwitterionic phosphonate−PEO−magnetite complex in DI water (black diamonds) and 0.17 M NaCl (open circles), and (B) the 8300 g mol^{-1} monozwitterionic phosphonate−PEO−magnetite complex in DI water (black diamonds) and 0.17 M NaCl (open circles).

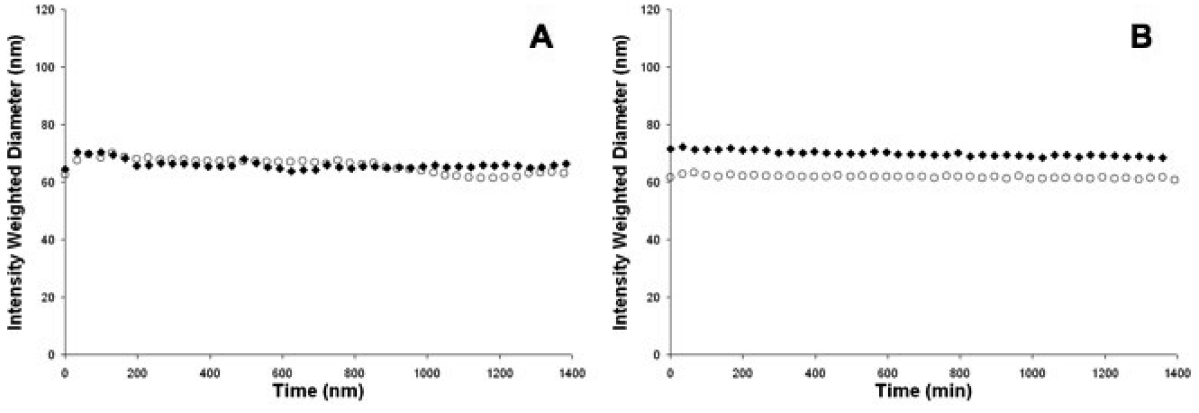

Figure 12. Intensity weighted diameters of the 3400 (open circles) and 9100 g mol^{-1} (black diamonds) trizwitterionic phosphonate−PEO−magnetite complexes in (A) DI water and (B) PBS over 24 h.

primarily attributed to high magnetite nanoparticle surface coverage. McDermott et al. performed quartz crystal microbalance experiments on octadecylphosphonate adsorbed onto SiO_2 in THF (a good solvent) and determined the footprint of the phosphonate group to be 18.5 Å^2.[33] Assuming this applies to our system, for a magnetite sphere with a radius of 4.0 nm there is 145 nm^2 of available surface area, or enough space for 734 zwitterionic phosphonate groups to adsorb. We can calculate the total number of chains per particle for each complex and then calculate how much of the available surface area is taken up by each chain depending on whether there are one or three zwitterionic phosphonate anchor groups. Assuming every zwitterionic

(33) McDermott, J. E.; McDowell, M.; Hill, I. G.; Hwang, J.; Kahn, A.; Bernasek, S. L.; Schwartz, J. *J. Phys. Chem. A* **2007**, *111*, 12333–12338.

phosphonate group is adsorbed on the surface, the 2900 and 8300 g mol^{-1} monozwitterionic phosphonate complexes and the 3400 and 9100 g mol^{-1} trizwitterionic phosphonate complexes have 83%, 36%, >100%, and >100% surface coverage, respectively. Thus, the complex with the most available magnetite surface area also shows aggregation in DI water (Figure 11B). At constant polymer loading, decreasing the PEO molecular weight increases the total number of chains and anchor groups and eliminates this aggregation in DI water. Moreover, by increasing the number of anchor groups 3-fold, the predicted surface coverage increases substantially, as do the stabilities of the complexes in both DI water and PBS. This shows that by increasing the total number of anchor groups, either through reduction of molecular weight (more chains nm^{-2}) or by increasing the number of anchor groups per chain (trizwitterionic phosphonate anchor group), the colloidal stability of these materials can be controlled in PBS.

We also suspect that the aggregation observed in DI water for complexes with the 8300 g mol^{-1} monozwitterionic phosphonate anchor group was likely due to an interaction between the magnetite of one complex and the anchor groups of another complex. Were this aggregation due to an interaction between anchor groups of different complexes, we would expect to observe more aggregation with an increase in the number of anchor groups. However, we see no aggregation of the trizwitterionic phosphonate complexes in DI water, and this indicates that the critical variable is not an interaction between anchor groups, but rather the availability of the magnetite surface.

Conclusions

It is clear that the phosphonate zwitterion end groups remain stably bound to the magnetite in either water or PBS, whereas the carboxylate and ammonium end groups allow the polymers to desorb in PBS. The colloidal instabilities of the carboxylate and ammonium complexes are attributed to polymer desorption from the surface of the magnetite nanoparticles in the presence of phosphate salts.[9]

The fact that PEO−magnetite complexes with phosphonate zwitterions remained stably bound in PBS allowed us to consider colloidal size stabilities in light of the density of chains, molecular weights of the bound chains and the predicted surface coverage (i.e., the possible footprint of a trifunctional vs monofunctional zwitterionic phosphonate chain). The improved colloidal size stability of complexes with the trizwitterionic phosphonate anchor groups is likely due to an increase in surface coverage associated with the multiple anchor groups. For a given polymer loading, the availability of the magnetite surface can also be reduced by shortening the polymer molecular weight, which increases the total number of adsorbed chains.

TGA data confirmed that neither of the novel monozwitterionic phosphonate or the trizwitterionic phosphonate-anchored polyethers desorbed from the magnetite surface upon exposure to PBS. Coupled with no measurable aggregation of the trizwitterionic phosphonate polyether-magnetite complexes in PBS, these seem to be the best-suited complexes for applications that occur in physiological conditions.

Acknowledgment. The authors are grateful for the financial support from NSF under Contract DMR-0805179. They are also grateful for measurements of the magnetic properties of these materials by M. R. J. Carroll and T. G. St. Pierre at the School of Physics, University of Western Australia. W. C.M. acknowledges partial support for this work by the Macromolecular Interfaces with Life Science IGERT of the NSF DGE-0333378.